

An effective proposal for strength evaluation of steel plates randomly corroded on both sides under uniaxial compression

Mohammad Reza Khedmati*, Zorareh Hadj Mohammad Esmaeil Nouri
and Mohammad Mahdi Roshanali

Faculty of Marine Technology, Amirkabir University of Technology, Tehran 15914, Iran

(Received November 30, 2009, Accepted March 04, 2011)

Abstract. This paper presents the results of an investigation into the post-buckling behaviour and ultimate strength of imperfect corroded steel plates used in ship and other marine-related structures. A series of elastic-plastic large deflection finite element analyses is performed on randomly corroded steel plates. The effects of general corrosion on both sides of the plates are introduced into the finite element models using a random thickness surface model. The effects on plate compressive strength as a result of parametric variation of the corroded surface geometry are evaluated. A proposal on the effective thickness is concluded in order to estimate the ultimate strength and explore the post-buckling behaviour of randomly corroded steel plates under uniaxial compression.

Keywords: steel plate; randomly distributed general corrosion; uniaxial compression; effective thickness

1. Introduction

Plates, in either un-stiffened or stiffened configurations, are the most important structural elements of thin-walled structures, such as ship and offshore structures, Fig. 1. Ship plates are generally subjected to several types of in-plane or lateral loads. The loads may be applied separately or in combination with each other. Among them, the in-plane loads are almost larger than the other types from the magnitude point of view. The in-plane loads may be tensile or compressive depending on the practical loading conditions. In design of ships and also offshore structures, it is essential to ensure that the structure has sufficient strength to sustain extreme loading conditions. Some limit states in hogging or sagging conditions for ship hull girder are schematically shown in Fig. 2. Strength of plates and stiffened plates are crucial for the overall structural capacity, in other words, for the ultimate strength of the whole structure.

On the other hand, corrosion and corrosion-related problems are considered to be the most important factors leading to age-related structural degradation of ships and many other types of steel structures. Corrosion has a harmful consequence from the safety point of view and can lead to thickness penetration, fatigue cracks, brittle fracture and unstable failure. These failures can imply a risk of loss of human

* Corresponding author, Associate Professor, E-mail: khedmati@aut.ac.ir

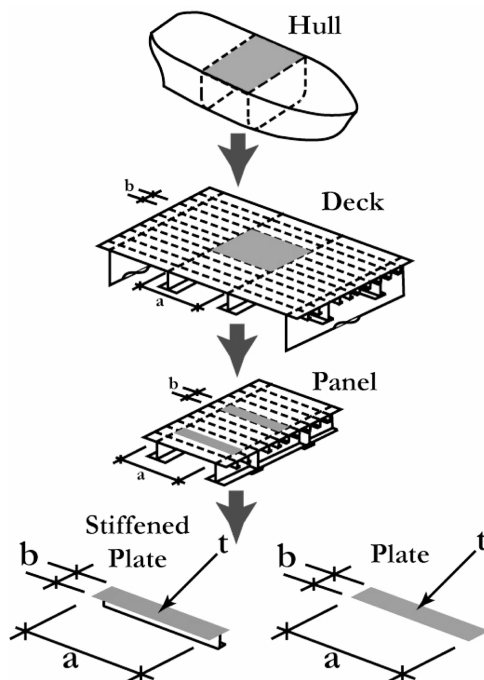


Fig. 1 Plate and stiffened plate elements

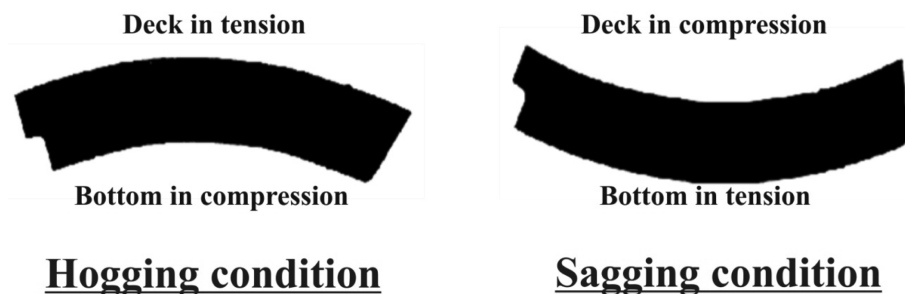


Fig. 2 Limit states in hogging or sagging conditions for a ship hull girder

lives and a risk of polluting the environment depending on the ship type, as happened in the case of tanker ship “*Energy Concentration*” (Fig. 3) in 1980.

Corrosion in ship structure is mainly observed in two distinct types, namely, general corrosion and localised corrosion. As an example of localised corrosion, reference may be made to the corrosion of hold frames in the way of cargo holds of bulk carriers which have a coating such as tar epoxy paints, Fig. 4 (Nakai et al. (2004)). Generally, pitting corrosion is defined as an extremely localised corrosive attack and sites of the corrosive attack are relatively small compared to the overall exposed surface (ASM Handbook (2001)). In the case of localised corrosion observed on hold frames of bulk carriers, the sites of the corrosive attack, i.e. pits, are relatively large (up to about 50 mm in diameter).

General corrosion is the problem when the plate elements such as the hold frames of bulk carriers have no protective coating, Fig. 5. Both surfaces of the plate may be corroded, in a pattern like the sea

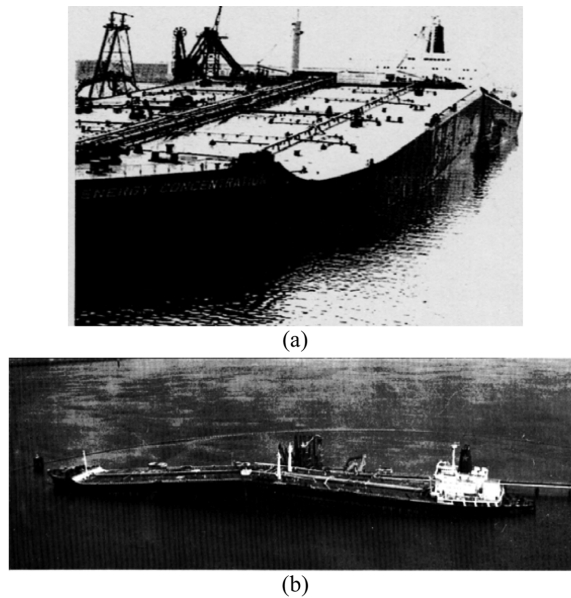


Fig. 3 Collapse of the tanker ship “Energy Concentration”: (a) Front view; (b) Longitudinal view

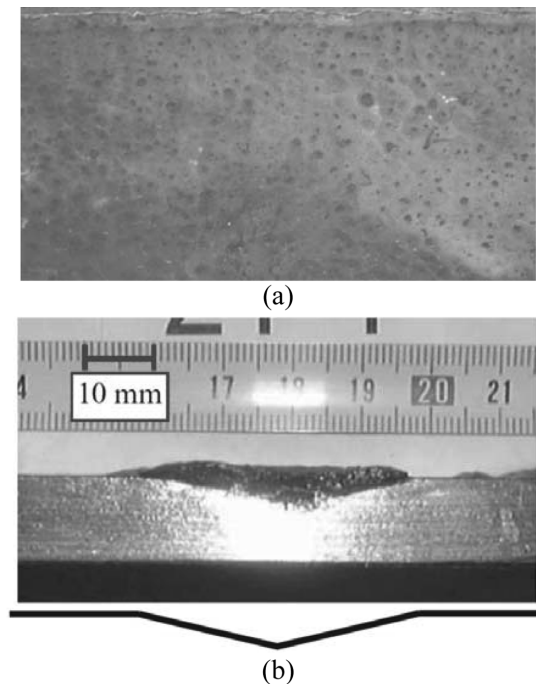


Fig. 4 Pitted web plate of the hold frame of a bulk carrier [1]: (a) Pitted surface; (b) Cross-sectional view

waves spectrum, as shown in Fig. 5.

Mateus and Witz (1997) investigated the effect of general corrosion on the post-buckling of plates using the uniform thickness reduction approach and a quasi-random thickness surface model. They

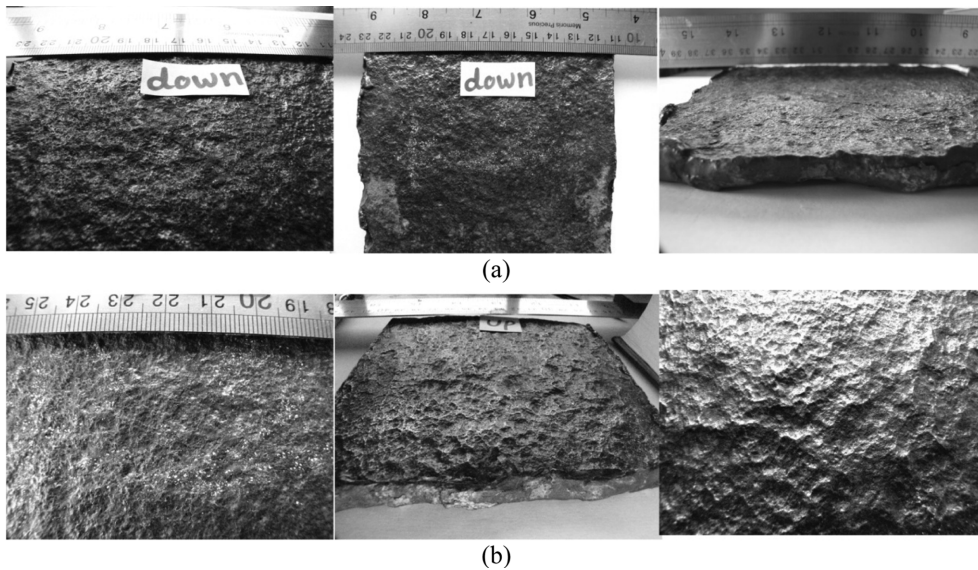


Fig. 5 Views on the surfaces of the plate suffering general corrosion

concluded that the usual uniform thickness reduction approach to account for general corrosion effects is not adequate because plastic hinges formed due to plate surface irregularity decrease the ultimate strength slightly and affects the post buckling behaviour of the plate significantly.

Daidola et al. (1997) proposed a mathematical model to estimate the residual thickness of pitted plates using the average and maximum values of pitting data or the number of pits and the depth of the deepest pit, and presented a method to assess the effect of thickness reduction due to pitting on local yielding and plate buckling based on the probabilistic approach. Furthermore, they developed a set of tools which can be used to assess the residual strength of pitted plates.

Slater et al. (2000) made a study on the buckling strength and behaviour of corroded ship plates using finite element method.

Paik et al. (2003 and 2004) studied the ultimate strength characteristics of pitted plate elements under axial compressive loads and in-plane shear loads, and derived closed form formulae for predicting the ultimate strength of pitted plates using the strength reduction (knock-down) factor approach. They dealt with the case where the shape of corrosion pits is a cylinder.

Ok et al. (2007) focused on assessing the effects of localised pitting corrosion which concentrates on one or several possibly large area on the ultimate strength of unstiffened plates. They applied the multi-variable regression method to derive new formulae to predict ultimate strength of unstiffened plates with localised corrosion. Their results indicated that the length, breadth and depth of pit corrosion have weakening effects on the ultimate strength of the plates while plate slenderness has only marginal effect on strength reduction. It was also concluded that the transverse location of pit corrosion is an important factor determining the amount of strength reduction.

Buckling or ultimate strength of corroded steel plates were investigated experimentally, numerically or analytically by some researchers (Cyr and Akhyas 2004, Akhyas and Cyr 2004, Nakai). Most of such studies were performed on the stiffened steel plates with pitted corrosion.

The main objective of the present paper is to examine how general corrosion affects the basic mechanical properties of plate members under compression and to explore the method of simulating

behaviour of plate members with general corrosion by FE analysis using shell elements.

Post-buckling behaviour and ultimate strength of imperfect corroded steel plates used in ships and other marine-related structures are studied in this paper. Elastic-plastic large deflection finite element analysis is carried out on the both sides of randomly corroded steel plates subject to uniaxial in-plane compression. General corrosion is modelled using a random thickness surface model. The influence of variations in the corroded surface geometry on the plate compressive strength is investigated. A simple formulation is proposed for the effective thickness of randomly corroded steel plates in order to estimate their ultimate strength and also explore their post-buckling behaviour under uniaxial compression.

2. Finite Element Analysis (FEA)

2.1 Extent of the model

The plates in ships and offshore structures are continuous. Longitudinal stiffeners and transverse frames divide the surface of the plates into isolated regions, Fig. 6(a). Such regions, which are shaded in Fig. 6(a), are considered as the model extent in the analyses.

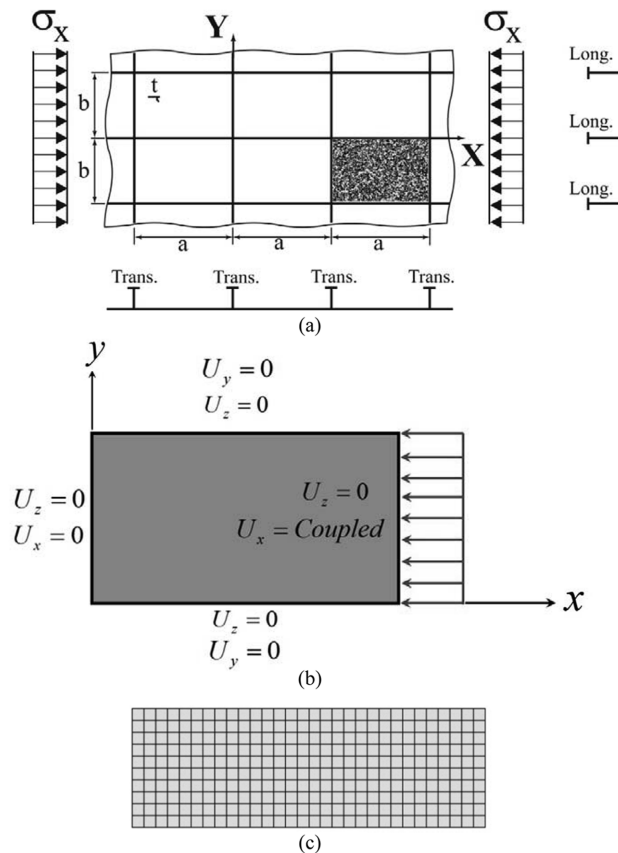


Fig. 6 (a) Extent of the model, (b) Boundary and loading conditions (c) Finite element discretisation

2.2 Loading and boundary conditions

As shown in Fig. 6(a), each region of the continuous plate is isolated by longitudinal stiffeners and transverse frames. To consider the effects of longitudinal stiffeners and transverse frames in the model of isolated plates, proper boundary conditions are to be applied on it. The description of applied boundary condition in the analyses is shown in Fig. 6(b). Loading would be compressive along x -axis of the Fig. 6(a).

2.3 Finite Element code, adopted element and mesh density

The ANSYS was used in all FE analyses. A code was prepared in APDL (ANSYS Parametric Design Language) to facilitate the parametric modelling and analysis using ANSYS (2008).

Plates are modelled by SHELL181 elements with elastic-plastic large deflection solution option. SHELL181 is suitable for analyzing thin to moderately-thick shell structures. It is a 4-node element with six degrees of freedom at each node: translations in the x , y , and z directions, and rotations about the x , y , and z -axes. SHELL181 is well-suited for linear, large rotation, and/or large strain nonlinear applications. Changes in shell thickness are accounted for in nonlinear analyses. In order to obtain reasonable results, a number of sensitivity analyses were carried out to find out the optimum mesh density and proper values of nonlinear analysis options. A sample of finite element discretisation is represented in Fig. 6(c), which is relevant to a plate of aspect ratio of 3 with 30 and 10 meshes seeding in the longitudinal and transverse directions, respectively.

2.4 Applied material properties

The material used in the models was of two different types: normal strength steel (abbreviated by *NS* steel) and high tensile strength steel (abbreviated by *HTS* steel), Fig. 7. Both types of steels have a Young's modulus of 21000 kgf/mm^2 and a Poisson's ratio of 0.3 . It is evident that strain-hardening effect has some influence on the nonlinear behaviour of plates. The degree of such an influence is a function of many factors including plate slenderness. In this study, material behaviour for plate was modelled in a bi-linear elastic-plastic manner with strain-hardening rate of $E/65$, Fig. 8. This value of strain-hardening rate was obtained through a large number of elastic-plastic large deflection analyses made by Khedmati (2000).

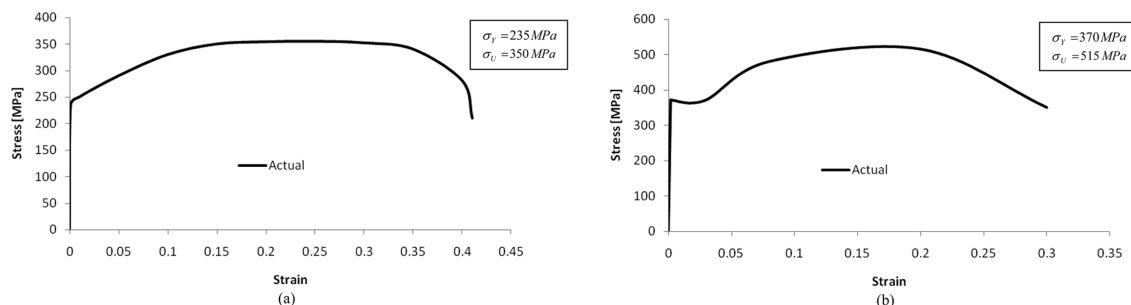


Fig. 7 Actual stress-strain curves: (a) NS steel; (b) HTS steel

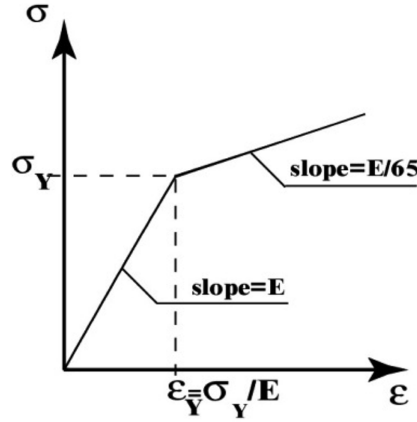


Fig. 8 Idealised bilinear model of stress-strain curve for material

2.5 Initial deflection and random general corrosion

The actual mode of the initial deflection of the plate is very complex, Fig. 9 (Fujikubo et al. (2005)). This complex mode can be expressed by a double sinusoidal series as

$$w_0 = \sum_{m=1}^{\infty} \sum_{n=1}^{\infty} A_{0mn} \sin \frac{m\pi x}{a} \sin \frac{n\pi y}{b} \quad (1)$$

When compressive load acts in the direction of the longer side of the plate (x -direction), the deflection components in the direction of the shorter side of the plate (y -direction) decrease with the increase in load except for the first term with one half-wave. In this case, only the first term ($n=1$) may play a dominant role, and the simpler form of the initial deflection can be used for the analysis as follows

$$w_0 = \sum_{m=1}^{\infty} A_{0m1} \sin \frac{m\pi x}{a} \sin \frac{\pi y}{b} \quad (2)$$

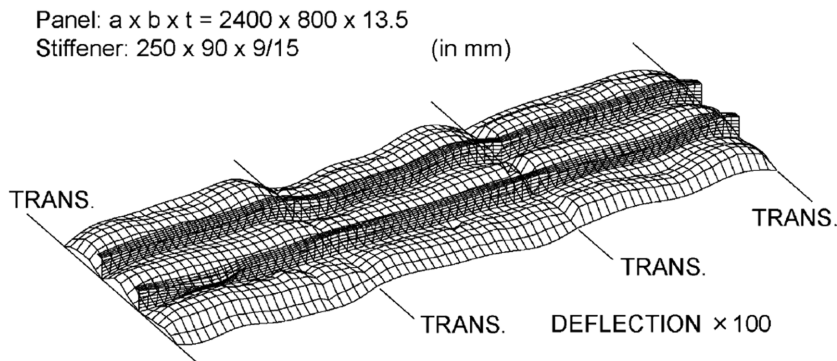


Fig. 9 Real distribution of initial deflection or so-called thin-horse mode initial deflection (Fujikubo et al. (2005))

Ueda and Yao (1985) used only odd terms. Finally, Yao et al. (1992) also introduced even terms into this mode, and the so-called *idealised thin-horse mode* took the following form:

$$w_0 = \sum_{m=1}^{11} A_{0m1} \sin \frac{m\pi x}{a} \sin \frac{\pi y}{b} \quad (3)$$

The initial deflection mode expressed by Eq. 3 is called *idealised thin-horse mode*, since the relevant deflection surface is similar in shape to the back of a thin horse. The coefficients of this mode are given in Table 1 (Yao et al. 1992) as functions of plate aspect ratio and its thickness. The maximum magnitude of initial deflection, w_{0max} , is taken as

$$w_{0max} = 0.05 \beta^2 t \quad (4)$$

where β is the slenderness parameter of the plate and defined by

$$\beta = \frac{b}{t} \sqrt{\frac{\sigma_Y}{E}} \quad (5)$$

where σ_Y and E are yield stress and modulus of elasticity of the plate, respectively.

A plate subject to general corrosion has a random distribution of thickness over its area. The likelihood of these variations in thickness to form plastic hinges that may affect the buckling and post-buckling behaviour of a corroded plate, and perhaps its ultimate strength, is something that cannot be discarded without further analysis.

It may be reasonable to assume that the corroded surfaces of a plate with its random thickness variation is composed of an infinite summation of random coefficients associated with each of the elastic buckling modes of the plate. Ohyagi's (1987) corrosion model is explained as

$$d_w = 0.34 n_y \quad (6)$$

where n_y is the number of years of exposure and d_w is the uniform reduction in thickness in millimeters after n_y years of exposure. The standard deviation associated with the normal distribution is 0.23 mm, based on the studies of Ohyagi (1987).

In numerical terms, the general corrosion model describes the typical surfaces of a corroded plate as a random thickness variation, t_p , with an average value equal to the original thickness of plate, minus the corroded equivalent thickness reduction. The following expression was applied in the studies made by Mateus and Witz (1987)

Table 1 Coefficients of thin-horse mode initial deflection as a functions of plate aspect ratio.

a/b	A_{01}/t	A_{02}/t	A_{03}/t	A_{04}/t	A_{05}/t	A_{06}/t	A_{07}/t	A_{08}/t	A_{09}/t	A_{010}/t	A_{011}/t
$1 < a/b < \sqrt{2}$	1.1158	-0.0276	0.1377	0.0025	-0.0123	-0.0009	-0.0043	0.0008	0.0039	-0.0002	-0.0011
$\sqrt{2} < a/b < \sqrt{6}$	1.1421	-0.0457	0.2284	0.0065	0.0326	-0.0022	-0.0109	0.001	-0.0049	-0.0005	0.0027
$\sqrt{6} < a/b < \sqrt{12}$	1.1458	-0.0616	0.3079	0.0229	0.1146	-0.0065	0.0327	0.000	0.000	-0.0015	-0.0074
$\sqrt{12} < a/b < \sqrt{20}$	1.1439	-0.0677	0.3385	0.0316	0.1579	-0.0149	0.0743	0.0059	0.0293	-0.0012	0.0062
$\sqrt{20} < a/b < \sqrt{30}$	1.1271	-0.0697	0.3483	0.0375	0.1787	-0.0199	0.0995	0.0107	0.0537	-0.0051	0.0256

$$t_p(x, y) = t - d_w + \sum_{i=1}^{\infty} \sum_{k=1}^{\infty} (A_i \cdot f_i(x) + B_k \cdot g_k(y)) \quad (7)$$

where A_i and B_k are the random coefficients associated with mode i in the x -direction and the mode k in the y -direction, respectively, and $f_i = \sin(i\pi x / a)$, $g_k = \sin(k\pi y / b)$. In this paper, randomly corroded surfaces were generated for both sides of the plate, instead of above-mentioned expression of double sinusoidal summation. A special purpose computer code was written in FORTRAN90. The generation of randomly corroded surfaces was achieved using the features of the DRANDM function of FORTRAN90. There was one limitation in the generation process and it was standard deviation of the plate thicknesses at different nodes that was set to 0.23 mm, as investigated by Ohyagi (1987). Finally, the z -coordinate of upper and lower surfaces of the plate can be defined as in Fig. 10(a)

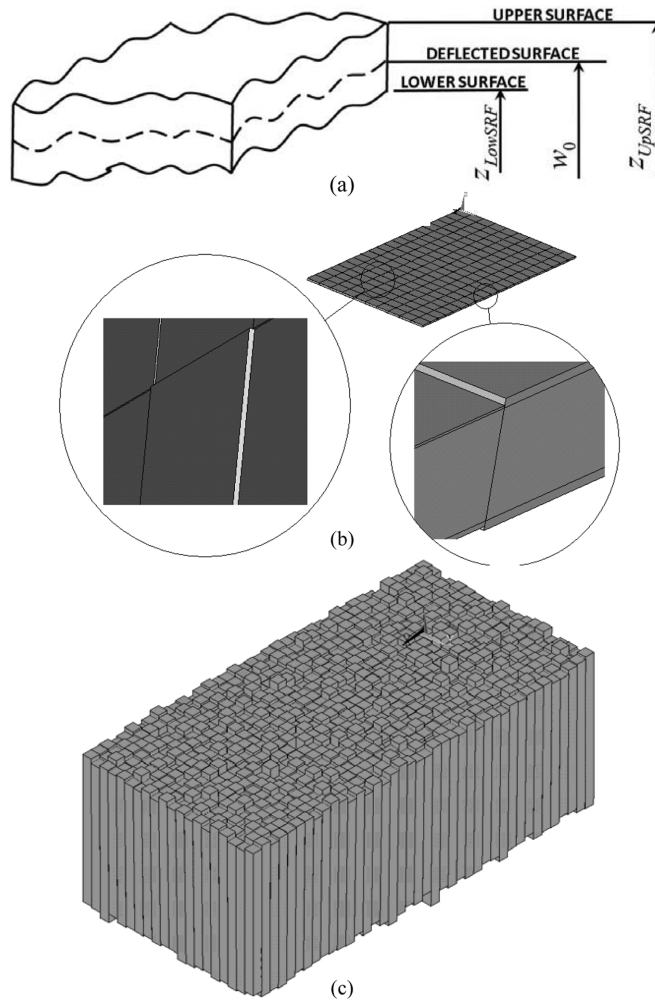


Fig. 10 Finite element analysis modeling details for general corrosion: (a) Different surfaces and relevant parameters; (b) Plate discretisation; (c) Perspective view of the randomly corroded plate with magnified thickness

$$z_{LowSRF} = w_o + \frac{t - d_w}{2} - r_1, \quad z_{UpSRF} = w_o + \frac{t - d_w}{2} + r_2 \quad (8)$$

where

$$t_p = z_{UpSRF} - z_{LowSRF} = t - d_w + r_1 + r_2 \quad (9)$$

And r_1 and r_2 are the random numbers, corresponding to the random thickness variation of the plate surfaces, produced by DRANDM function.

There are several finite element techniques available to model uniform corrosion. The easiest way is to reduce the thickness of the plate in surface, to carry out buckling analysis to get the buckled shape of plate with uniform corrosion and finally to perform nonlinear finite element control to get the ultimate strength of plate by using stress versus strain relationship. Khedmati and Karimi (2006) modelled the corroded plate with 3-D 20-node structural solid element but this method also cannot represent the real situation and easily tends to fail to converge during nonlinear control according to the author's experience.

Figure 10(b) represents the modelling details in finite element analysis while Fig. 10(c) shows a magnified view of the plate with surfaces simulating random corrosion.

2.6. Validation

Various unstiffened and stiffened plate models in uncorroded condition have been tested experimentally by Ghavami (1994). All stiffened plate models were successfully simulated by Ghavami and Khedmati (2006). Two of the models tested by Ghavami were of unstiffened type. A view on the test rig used by Ghavami (1994) is shown in Fig. 11. Table 2 summarises the specifications of the unstiffened plate models tested by Ghavami (1994) and also their ultimate strength characteristics. The ultimate strength values obtained by numerical simulation using finite element method (FEM) are given in Table 2. As can be seen from Table 2, the obtained experimental and numerical results show very good correlation. Upon such successful agreements, numerical simulations are extended here on the corroded models.

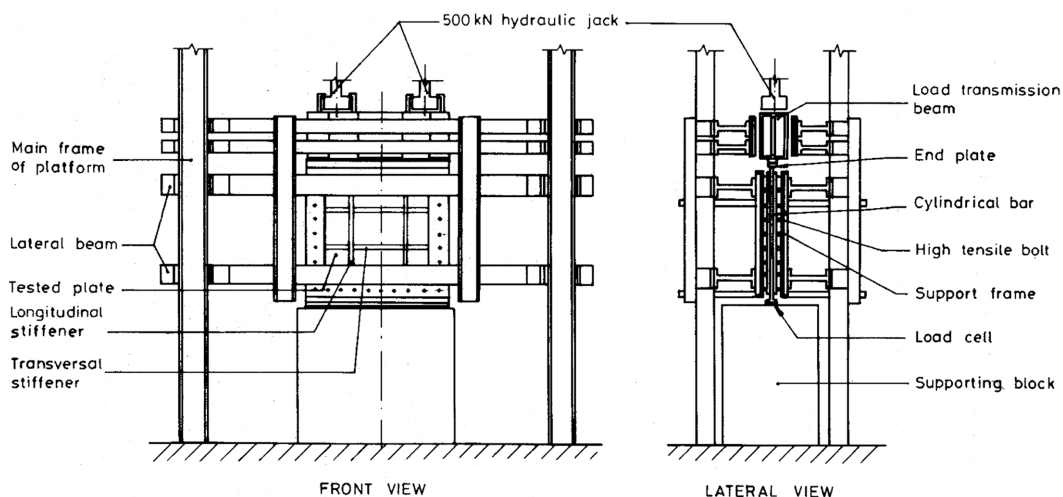


Fig. 11 Ghavami's (1994) testing rig

Table 2 Specifications of plate models tested by Ghavami (1994) and their strength characteristics

Test model	Plate			Material properties		Ultimate strength		
	a	b	t	E	σ_Y	$(\sigma_{Ult})_{Test} / \sigma_Y$	$(\sigma_{Ult})_{FEM} / \sigma_Y$	$(\sigma_{Ult})_{FEM} / (\sigma_{Ult})_{Test}$
	mm	mm	mm	MPa $\times 10^5$	MPa	%	%	%
P1	650	650	4.4	1.81	218	42.2	36.7	0.87
P2	650	650	4.8	1.78	220	48.2	50.6	1.05

3. Parametric study

In order to study the effects of random thickness variation on the response of axially loaded plates, different cases were considered. The cases included in the study are briefly explained as follows:

- Corroded plates with $AR = 2$, $t = 14$ mm, mean corrosion depth = 2 mm and $S = 0.2$ made of *HTS* steel
- Corroded plates with $AR = 3$, $t = 14$ mm, mean corrosion depth = 2 mm and $S = 0.2$ made of *HTS* steel
- Corroded plates with $AR = 2$, $t = 18$ mm, mean corrosion depth = 2 mm and $S = 0.2$ made of *HTS* steel
- Corroded plates with $AR = 3$, $t = 18$ mm, mean corrosion depth = 2 mm and $S = 0.2$ made of *HTS* steel
- Corroded plates with $AR = 2$, $t = 14$ mm, mean corrosion depth = 2 mm and $S = 0.2$ made of *NS* steel
- Corroded plates with $AR = 3$, $t = 14$ mm, mean corrosion depth = 2 mm and $S = 0.2$ made of *NS* steel
- Corroded plates with $AR = 2$, $t = 18$ mm, mean corrosion depth = 2 mm and $S = 0.2$ made of *NS* steel
- Corroded plates with $AR = 3$, $t = 18$ mm, mean corrosion depth = 2 mm and $S = 0.2$ made of *NS* steel.

For each of the above cases, 50 models were created changing the random thickness variation parameters. The corroded surfaces of the models were different in these cases. Gaussian distribution for random thickness variation was considered in all cases and corresponding models. All of the plate models were analysed under longitudinal in-plane compression. Average stress-average strain relationships for the models are shown in Figs. 12, 13, 14, 15, 16, 17, 18 and 19, respectively. The maximum magnitude of thin-horse mode initial deflection for the corroded models is calculated using Eq. 4 for the

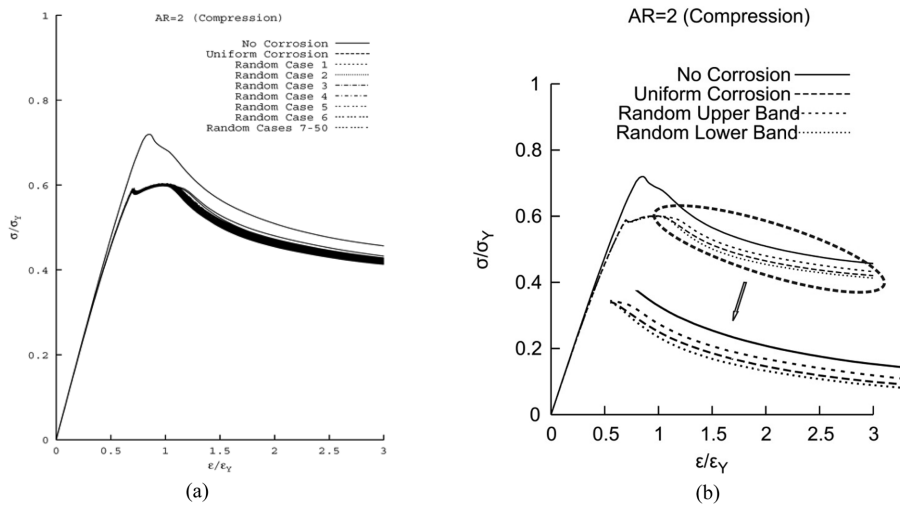


Fig. 12 Comparison of average stress-average strain relationships for corroded plates with $AR = 2$, $t = 14$ mm, mean corrosion depth = 2 mm and $S = 0.2$ made of *HTS* steel

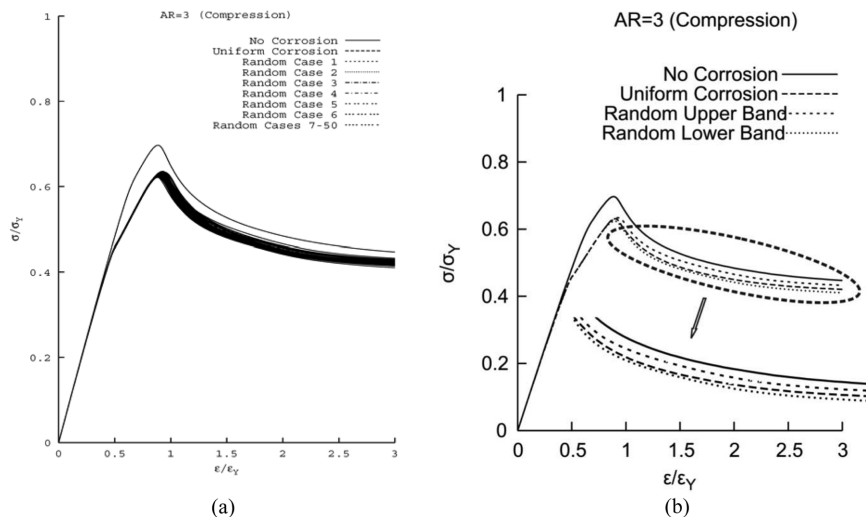


Fig. 13 Comparison of average stress-average strain relationships for corroded plates with $AR = 3$, $t = 14$ mm, mean corrosion depth = 2 mm and $S = 0.2$ made of HTS steel

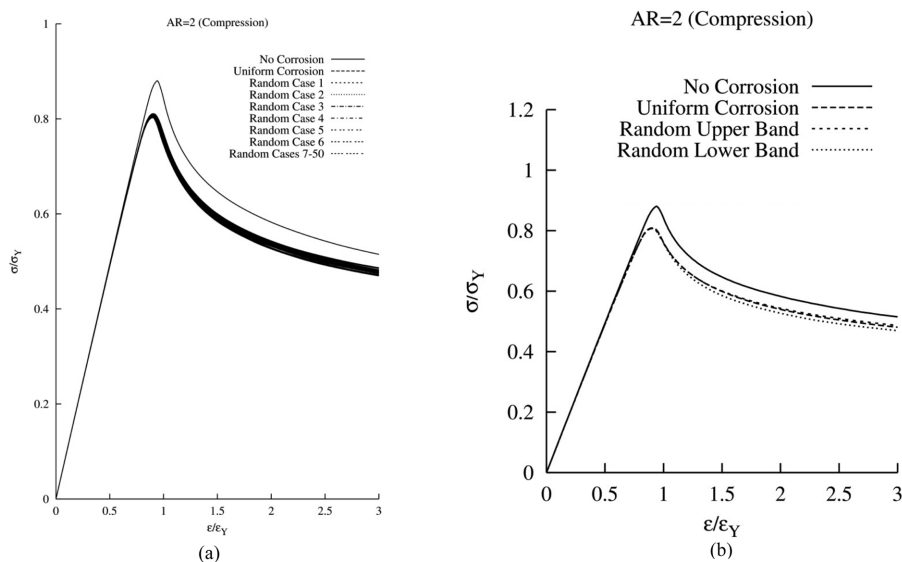


Fig. 14 Comparison of average stress-average strain relationships for corroded plates with $AR = 2$, $t = 18$ mm, mean corrosion depth = 2 mm and $S = 0.2$ made of HTS steel

original thickness. Also, Von Mises stress distributions are shown for a selection of the cases in Tables 3, 4, 5, 6 and 7. A summary of values of the buckling strength, ultimate strength and reserve strength for all models is given in Table 8. Sample perspective views on the surfaces of a plate with random Gaussian distribution of corrosion are shown in Fig. 20.

The average stress-average strain relationships of the plate models in un-corroded condition as well

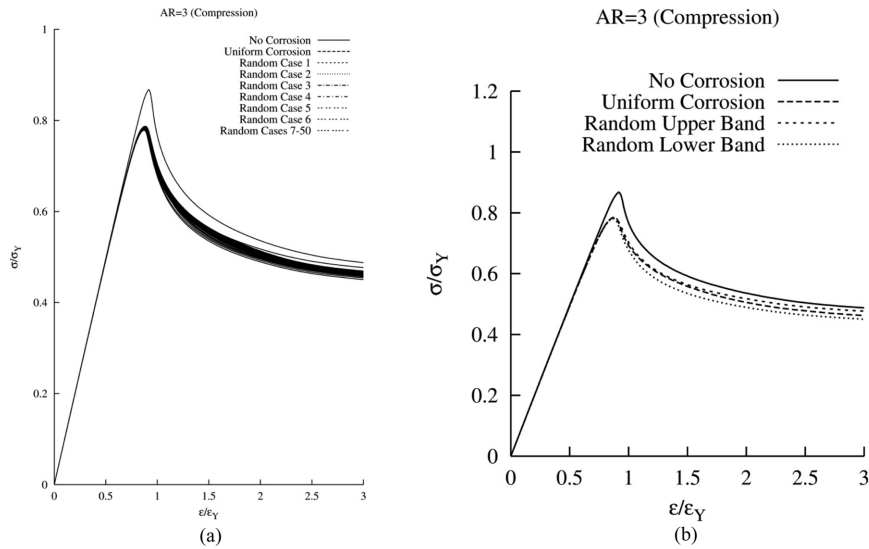


Fig. 15 Comparison of average stress-average strain relationships for corroded plates with $AR = 3$, $t = 18$ mm, mean corrosion depth = 2 mm and $S = 0.2$ made of HTS steel

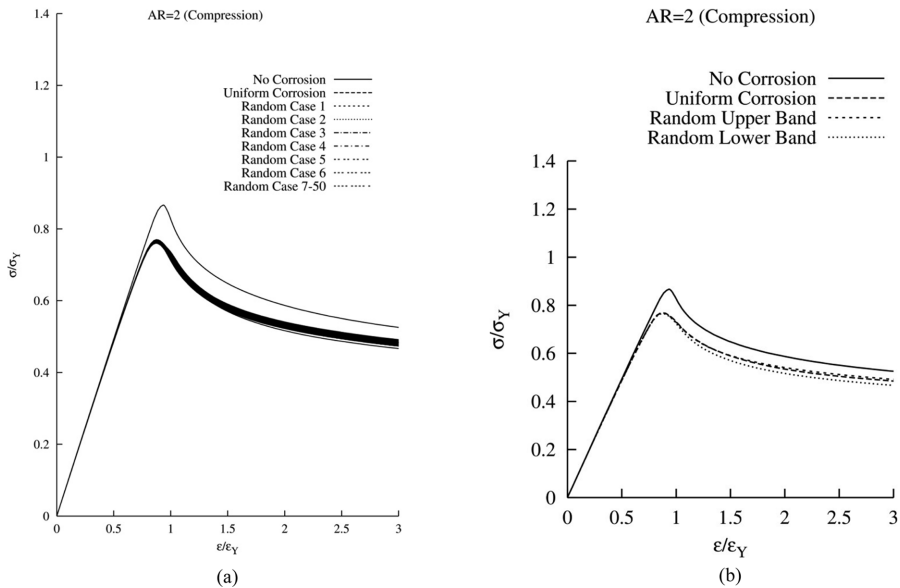


Fig. 16 Comparison of average stress-average strain relationships for corroded plates with $AR = 2$, $t = 14$ mm, mean corrosion depth = 2 mm and $S = 0.2$ made of NS steel

as in the condition of having uniform thickness reduction are shown in Figs 12 to 19. The plate in the condition of uniform corrosion or uniform thickness reduction has a reduction equal to the mean corrosion depth from its original un-corroded thickness.

Figures 12 to 19, in addition to the results summarised in Tables 3 to 8, reveal the following main

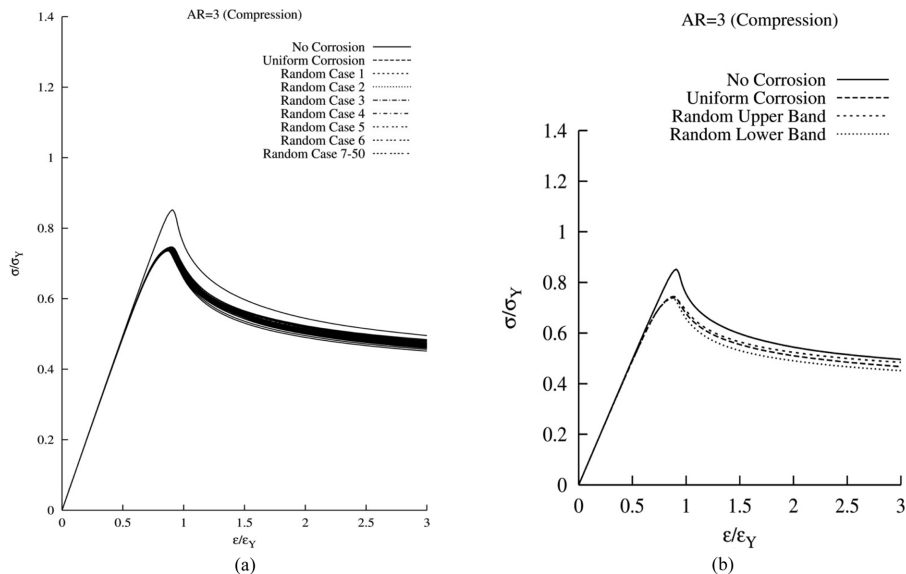


Fig. 17 Comparison of average stress-average strain relationships for corroded plates with $AR = 3$, $t = 14$ mm, mean corrosion depth = 2 mm and $S = 0.2$ made of NS steel

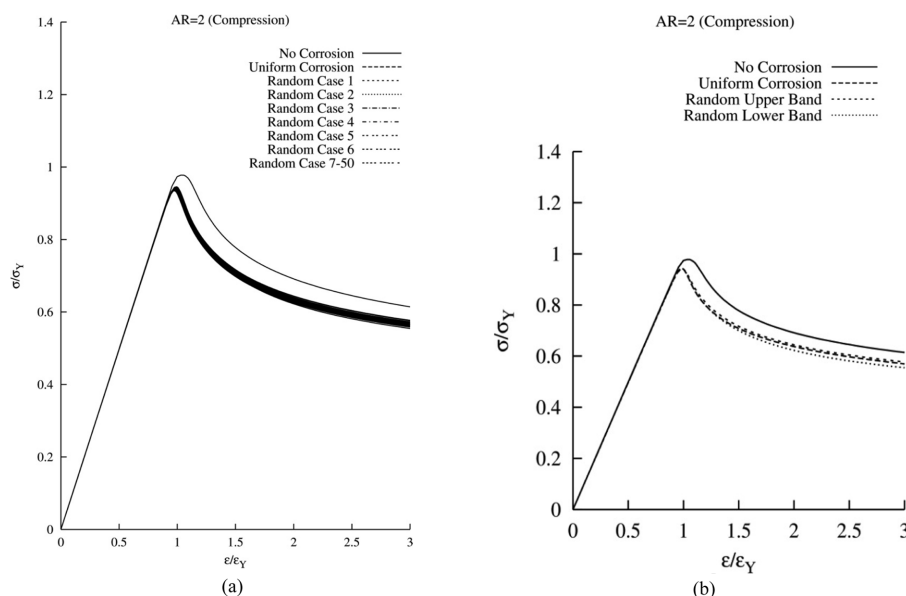


Fig. 18 Comparison of average stress-average strain relationships for corroded plates with $AR = 2$, $t = 18$ mm, mean corrosion depth = 2 mm and $S = 0.2$ made of NS steel

characteristics for the buckling/ultimate strengths and behaviours of the corroded plate models

- Random thickness variations in the plate model surfaces mainly affect their post-ultimate-strength regimes while their pre-ultimate-strength behaviours are almost unchanged.
- The buckling and ultimate strengths for any group of 50 models analysed in each of the above-

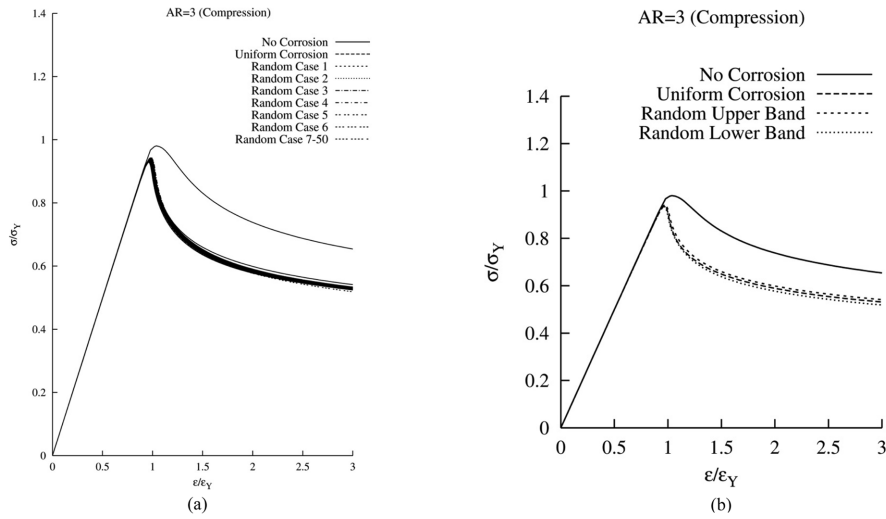


Fig. 19 Comparison of average stress-average strain relationships for corroded plates with $AR = 3$, $t = 18$ mm, mean corrosion depth = 2 mm and $S = 0.2$ made of NS steel

Table 3 Von-Mises stress contours for 14 mm plate models of aspect ratio of 2, made of HTS steel

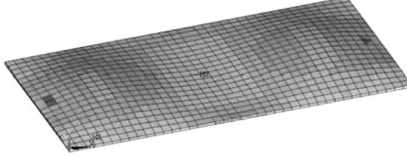
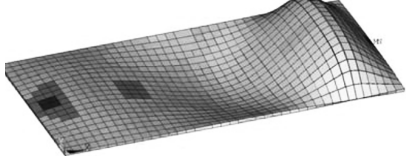
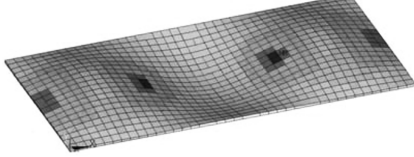
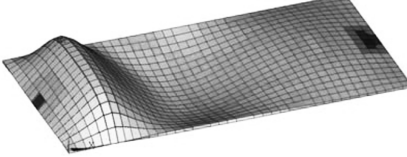
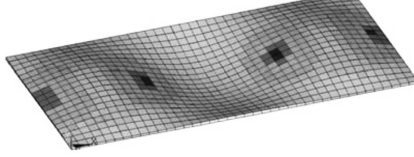
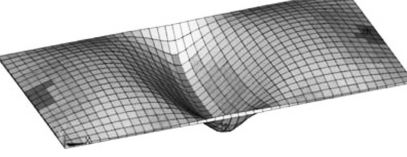
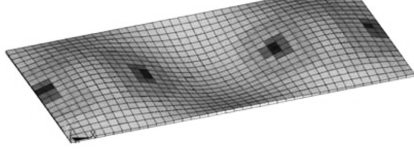
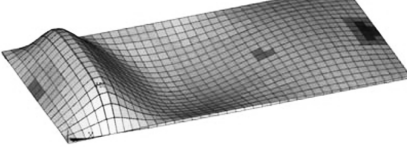
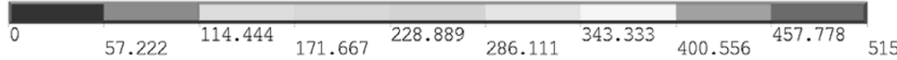
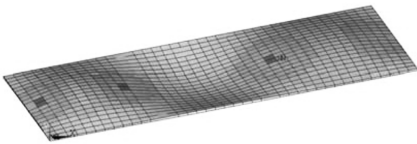
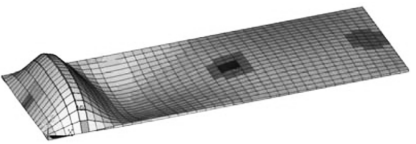
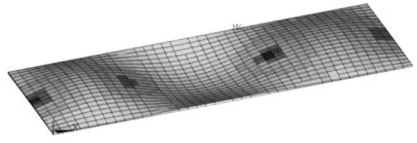
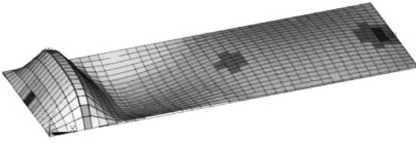
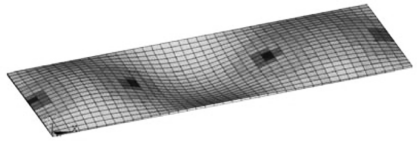
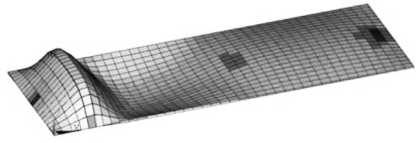
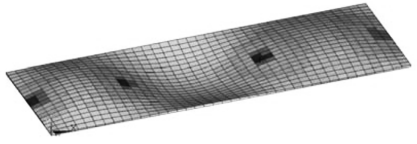
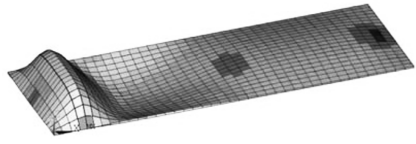
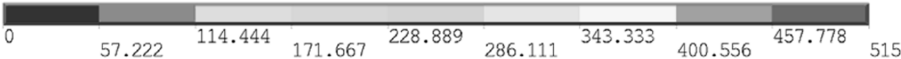
Plate $1600 \times 800 \times 14$, $W_{0max} = 0.05\beta^2t$, 2 mm corrosion				
Case	Ultimate strength step	$\frac{\sigma_{ave}}{\sigma_Y}$	Final step $\frac{\epsilon}{\epsilon_Y} = 3$	$\frac{\sigma_{ave}}{\sigma_Y}$
No. corrosion		0.720		0.457
Uniform corrosion		0.600		0.418
Random upper band		0.601		0.431
Random lower band		0.599		0.412
				

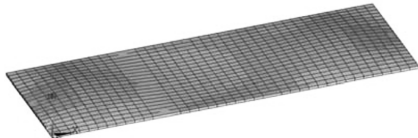
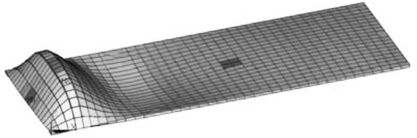
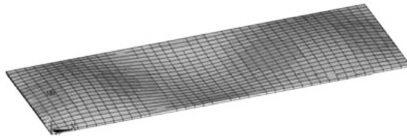
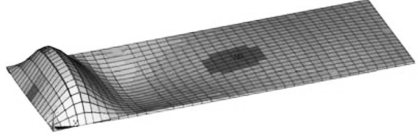
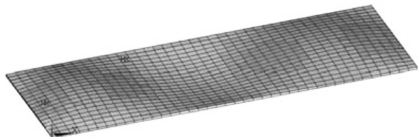
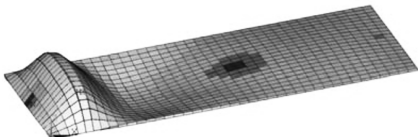
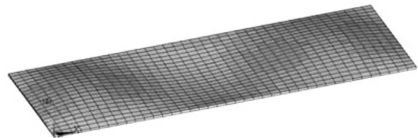
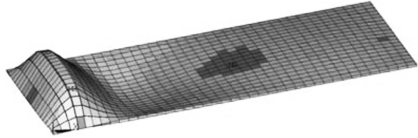
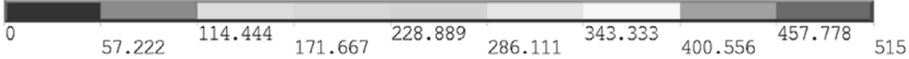
Table 4 Von-Mises stress contours for 14 mm plate models of aspect ratio of 3, made of HTS steel.

Plate $2400 \times 800 \times 14$, $W_{0max} = 0.05\beta^2t$, 2 mm corrosion				
Case	Ultimate strength step	$\frac{\sigma_{ave}}{\sigma_Y}$	Final step $\frac{\varepsilon}{\varepsilon_Y} = 3$	$\frac{\sigma_{ave}}{\sigma_Y}$
No corrosion		0.697		0.447
Uniform corrosion		0.631		0.420
Random upper band		0.634		0.432
Random lower band		0.624		0.410
				

mentioned cases are almost insensitive to the random thickness variations over the plate surfaces.

- Random thickness variation scheme applied to the plate surfaces has led to a reduction in the buckling and ultimate strengths of the models. The amount of reduction is a function of plate aspect ratio, plate thickness (slenderness parameter) and also the plate material.
- By changing the type of material from HTS steel to NS steel, the amounts of reductions in the buckling strengths are generally diminished. The difference between the buckling strengths of corroded plate models with that of their corresponding un-corroded condition is in the ranges of 17-37 percent and 4-18 percent in cases of using HTS or NS steels, respectively.
- Besides, the difference between the ultimate strengths of corroded plate models with that of their corresponding un-corroded condition is in the ranges of 5-26 percent without any specific trend. The main parameter influencing this reduction seems to be the plate slenderness parameter or thickness. The thicker the plate, the less the reduction in the ultimate strength of the corroded plate model in comparison with its corresponding un-corroded condition.
- For any group of the 50 analysed plate models in each of above-mentioned cases, the post-ultimate-strength regions of the average stress-average strain relationships create a band. The band width is generally decreased with changing the plate aspect ratio from 3 to 2.
- The curve of average stress-average strain for the condition of uniformly corroded plate model lies

Table 5 Von-Mises stress contours for 18 mm plate models of aspect ratio of 3, made of HTS steel

Plate $2400 \times 800 \times 18$, $W_{0max} = 0.05\beta^2t$, 2 mm corrosion				
Case	Ultimate strength step	$\frac{\sigma_{ave}}{\sigma_Y}$	Final Step $\frac{\varepsilon}{\varepsilon_y} = 3$	$\frac{\sigma_{ave}}{\sigma_Y}$
No corrosion		0.868		0.488
Uniform corrosion		0.785		0.462
Random upper band		0.783		0.477
Random lower band		0.781		0.450
				

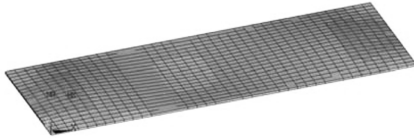
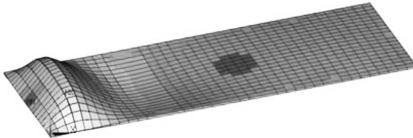
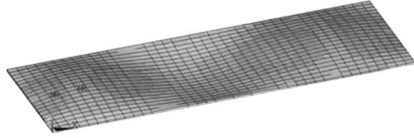
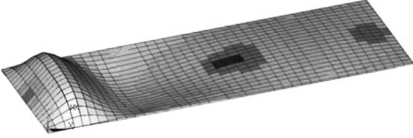
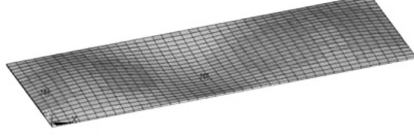
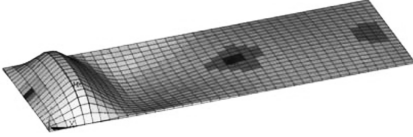
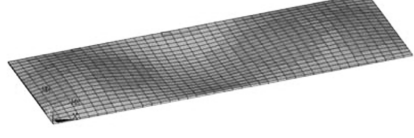
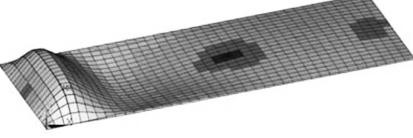
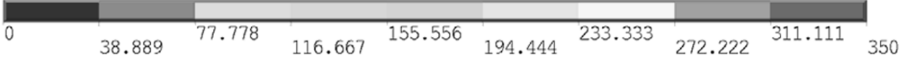
inside the band of average stress-average strain relationships of corresponding randomly corroded models. This can be well understood by paying attention to Figs. 12(b) to 19(b) where the curve of uniformly corroded plate model is seen to be in between the curves, corresponding to upper and lower limits of the bands in each of the analysed cases.

- In each case, the trends of the curves in the post-ultimate-strength region are similar.
- The mode shapes and Von Mises stress contours shown in Tables 3 to 7 reveal that almost regular half-waves are generated inside the plate extent in longitudinal direction at the ultimate strength level. Besides, post-ultimate-strength mode shapes show the local accumulation of deflection in some regions of the plate model in addition to the unloading the rest of plate area. The place of local deflection accumulation is not fixed and, in other words, changes from case to case.

4. Proposal on effective thickness

Based on the results given in Figs. 12 to 19 and above-mentioned descriptions, the following equation is proposed as the effective thickness of the plate having random corrosion, for practical evaluation of its average stress-average strain relationship and strength characteristics

Table 6 Von-Mises stress contours for 14 mm plate models of aspect ratio of 3, made of NS steel

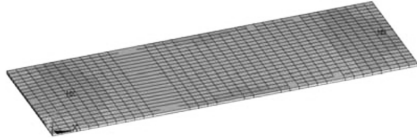
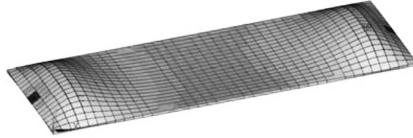
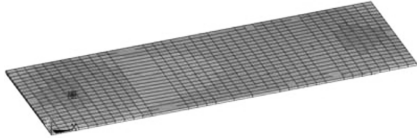
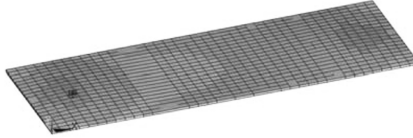
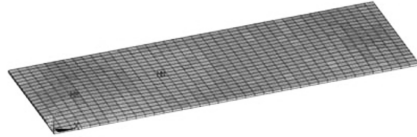
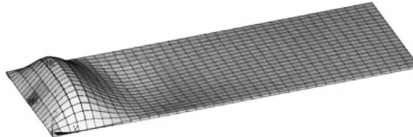
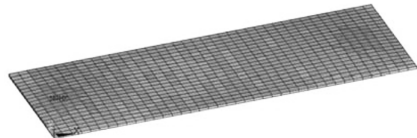
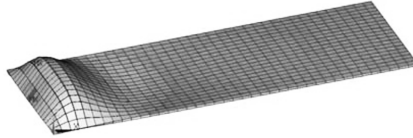
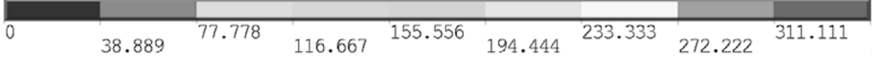
Plate $2400 \times 800 \times 14$, $W_{0max} = 0.05\beta^2t$, 2 mm corrosion				
Case	Ultimate strength step	$\frac{\sigma_{ave}}{\sigma_Y}$	Final step $\frac{\varepsilon}{\varepsilon_y} = 3$	$\frac{\sigma_{ave}}{\sigma_Y}$
No corrosion		0.852		0.494
Uniform corrosion		0.744		0.466
Random upper band		0.779		0.483
Random lower band		0.738		0.450
				

$$t_{eq} = t - \mu - S \quad (10)$$

Figures 21(a) and 21(b) give some explanations for the usefulness of applying the above equation. The plate under consideration in these figures has a length of 2,400 mm, breadth of 800 mm, original un-corroded thickness of 18 mm and is made of HTS steel. It is assumed that the plate has a random Gaussian distribution of corrosion on its both surfaces. The mean corrosion depth is assumed to be either 2 mm (Fig. 21(a)) or 4 mm (Fig. 21(b)). Standard deviation of the Gaussian distribution of random thickness is set to 0.4. Four average stress-average strain curves are seen in either Fig 21(a) or 21(b). The description of these four curves is as follows:

- Solid line: corresponding to the plate with uniform corrosion. This means that the plate has a thickness equal to its original thickness (18 mm) minus mean corrosion depth. The maximum magnitude of thin-horse mode initial deflection is calculated using Eq. 4 for the original thickness (18 mm).
- Dashed line: corresponding to the lower band or limit curve for the plate with random Gaussian distribution of corrosion. The maximum magnitude of thin-horse mode initial deflection is calculated using Eq. 4 for the original thickness (18 mm).
- Short-dashed line: corresponding to the plate with uniform corrosion. This means that the plate has a thickness equal to its original thickness (18 mm) minus mean corrosion depth. The maximum magnitude of thin-horse mode initial deflection is calculated using Eq. 4 for the uniformly corroded

Table 7 Von-Mises stress contours for 18 mm plate models of aspect ratio of 3, made of NS steel

Plate $2400 \times 800 \times 18$, $W_{0max} = 0.05\beta^2t$, 2 mm corrosion				
Case	Ultimate strength step	$\frac{\sigma_{ave}}{\sigma_Y}$	Final step $\frac{\epsilon}{\epsilon_y} = 3$	$\frac{\sigma_{ave}}{\sigma_Y}$
No corrosion				
Uniform corrosion				
Random upper band				
Random lower band				
				

thickness.

- Dotted line: corresponding to the plate with equivalent or effective thickness. The maximum magnitude of thin-horse mode initial deflection is calculated using Eq. 4 for the effective thickness.

As can be seen from Figs. 21(a) and 21(b), the average stress-average strain relationship derived using the effective thickness (based on Eq. 10) agrees well with that obtained for the other cases. Also, applying the effective thickness proposal in Eq. 10, the ultimate strength of the randomly corroded plate can be easily estimated based on the following set of equations (Fujikubo et al. (1999))

$$\frac{\sigma_{Ult}}{\sigma_Y} = \begin{cases} 1.0 & \text{for } \beta \leq 1.73 \\ 0.1 + \frac{1.571}{\beta} & \text{for } \beta > 1.73 \end{cases} \quad (11)$$

where β is to be calculated using the effective thickness of the corroded plate.

5. Conclusions

A series of nonlinear elastic-plastic finite element analyses has been performed on the plates in

Table 8 Comparison of results for all plate models.

· Plate aspect ratio · Plate thickness · Plate material	Corrosion condition	Buckling strength σ_{Cr} / σ_Y	Ultimate strength σ_{Ult} / σ_Y	Reserve strength at $\varepsilon / \varepsilon_Y = 3$
· $AR = 2$ · $t = 14$ mm · HTS steel	Uncorroded	0.600	0.719	0.457
	Corroded (mean corrosion depth = 2 mm, $S = 0.2$)	0.390	0.600	0.425
· $AR = 3$ · $t = 14$ mm · HTS steel	Uncorroded	0.590	0.697	0.447
	Corroded (mean corrosion depth = 2 mm, $S = 0.2$)	0.430	0.612	0.415
· $AR = 2$ · $t = 18$ mm · HTS steel	Uncorroded	0.847	0.880	0.515
	Corroded (mean corrosion depth = 2 mm, $S = 0.2$)	0.700	0.807	0.485
· $AR = 3$ · $t = 18$ mm · HTS steel	Uncorroded	0.800	0.868	0.500
	Corroded (mean corrosion depth = 2 mm, $S = 0.2$)	0.650	0.780	0.447
· $AR = 2$ · $t = 14$ mm · NS steel	Uncorroded	0.800	0.867	0.526
	Corroded (mean corrosion depth = 2 mm, $S = 0.2$)	0.520	0.768	0.479
· $AR = 3$ · $t = 14$ mm · NS steel	Uncorroded	0.809	0.852	0.496
	Corroded (mean corrosion depth = 2 mm, $S = 0.2$)	0.590	0.739	0.468
· $AR = 2$ · $t = 18$ mm · NS steel	Uncorroded	0.940	0.978	0.650
	Corroded (mean corrosion depth = 2 mm, $S = 0.2$)	0.910	0.941	0.566
· $AR = 3$ · $t = 18$ mm · NS steel	Uncorroded	0.967	0.981	0.654
	Corroded (mean corrosion depth = 2 mm, $S = 0.2$)	0.910	0.937	0.530

different conditions of un-corroded, uniformly corroded and randomly corroded. The plates have been subjected to in-plane compression load. Full-range average stress-average strain relationships of the plates have been derived considering the changes in plate aspect ratio, plate slenderness or thickness, mean corrosion depth and standard deviation of random thickness variation. The results can be summarised as follows:

Aspect ratio, thickness and also random corrosion parameters have different effects on the strength characteristics of the corroded plate. Random corrosion has the weakening effects on the buckling and ultimate strengths of the plate. The case of uniform corrosion leads to an intermediate condition for the plate with different probable random thickness variations.

In order to investigate the strength characteristics of the randomly corroded plate under the longitudinal in-plane compression, without any modelling of the random thickness variations, a practical proposal was developed to calculate the effective thickness of the plate.

It should be mentioned that the model used in this study is based on the concept of correlation. The collapse of the plates is generally sensitive to (a) local points of extreme weakness such as might come from the pitting and (b) correlated areas of reduced thickness. When considering such local weaknesses or correlations of reduced thickness inside the plate, other phenomena like local plastic hinges are

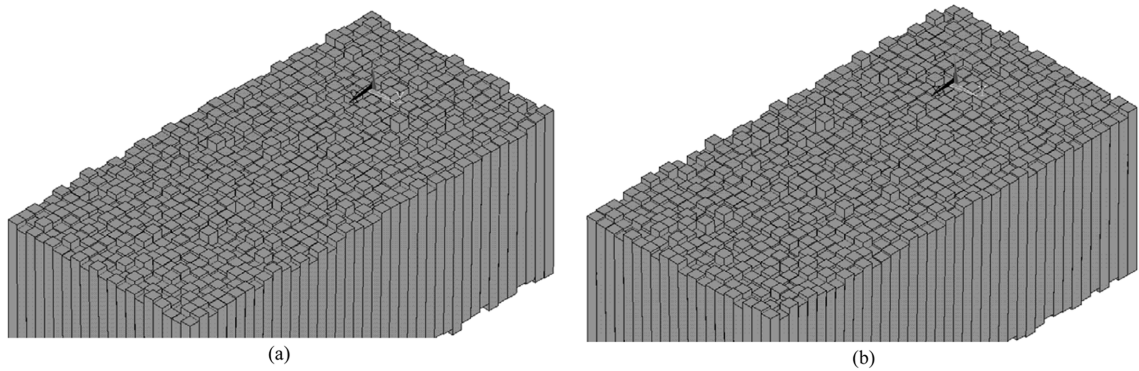


Fig. 20 Perspective views on the surfaces of the plate with random Gaussian distribution of corrosion ($AR = 2$, $t = 14$ mm, mean corrosion depth = 2 mm, $S = 0.2$ and made of HTS steel): (a) Lower band; (b) Upper band

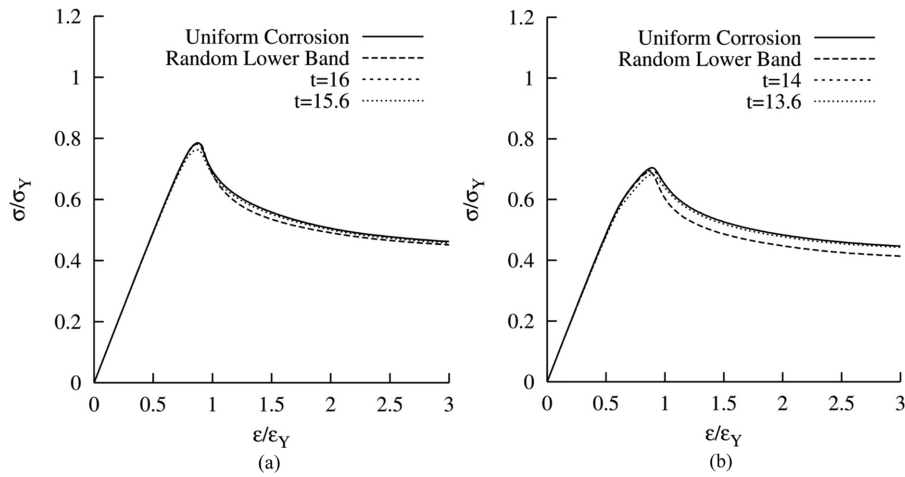


Fig. 21 Comparison of average stress-average strain relationships for a plate with random Gaussian distribution of corrosion ($a = 2400$ mm, $b = 800$ mm, $t = 18$ mm, mean corrosion depth = 2 and 4 mm, $S = 0.4$ and made of HTS steel): (a) Mean corrosion depth = 2 mm; (b) Mean corrosion depth = 4 mm

observed in addition to the usual buckling and collapse of the plate. Besides, assuming corrosion is uncorrelated leads to the notion that only the mean reduction matters. As a result of this assumption, localised buckling, localised collapse and localised plastic deformation may happen in small regions of the models (as shown in the Tables 3, 4, 5, 6 and 7). If correlation inside the areas of reduced thickness or among local points of extreme weakness is included in the thickness reduction scheme, then far greater variation in the obtained results will be expected to be seen. Therefore, a deeper and more thorough investigation for exploring buckling and collapse modes of the models in the presence of such correlations is needed. These remain as future works.

Notations

AR	Aspect ratio of the plate
a	Plate length
b	Plate breadth
t	Thickness of plate in un-corroded condition
t_{ef}	Effective thickness of plate in corroded condition
tp	Thickness function of plate in corroded condition
E	Young modulus of material
ν	Poisson's ratio of material
m	Number of half-waves in longitudinal direction
n	Number of half-waves in transverse direction
β	Plate slenderness
u	Mean corrosion depth
S	Standard deviation of random thickness variations
n_y	Number of years of exposure
d_w	Uniform reduction in thickness
r_1, r_2	Random numbers corresponding to the corroded surfaces of the plate
z_{upSRF}	Z-coordinate of the upper surface of the plate
z_{LowSRF}	Z-coordinate of the lower surface of the plate
U_x	Displacement along X-axis
U_y	Displacement along Y-axis
U_z	Displacement along Z-axis
A_{0mn}	Coefficients in initial deflection function
W_0	Initial deflection function
W_{0max}	Maximum magnitude of initial deflection
ε	Strain
ε_Y	Material yield strain
σ	Stress
σ_{Cr}	Buckling strength of the plate
σ_Y	Material yield stress
σ_U	Material ultimate stress
σ_{Ult}	Ultimate strength of the plate

References

- Nakai, T., Matsushita, H., Yamamoto, N., et al. (2004), "Effect of pitting corrosion on local strength of hold frames of bulk carriers (1st report)", *Mar. Struct.*, **17**, 403-432.
- ASM International Corrosion. (2001), "ASM Handbook", vol. 13.
- Mateus, A.F. and Witz, J.A. (1997), "On the post-buckling of corroded steel plates used in marine structures", *Trans. RINA*, **140**, 165-83.
- Daidora, J.C., Parente, J., Orisamololu, I.R., Ma K.T. (1997), "Residual strength assessment of pitted plate panels", Ship Structure Committee, SSC-394.

- Slater, P.A., Pandey, M.D. and Sherbourne, A.N. (2000), "Finite element analysis of buckling of corroded ship plates", *Can. J. Civ. Eng. CSCE*, **27**, 463-74.
- Paik, J.K., Lee, J.M. and Ko, M.J. (2003), "Ultimate compressive strength of plate elements with pit corrosion wastage", *J. Eng. Mar. Environ.*, **217**(M4), 185-200.
- Paik, J.K., Lee, J.M. and Ko, M.J. (2004), "Ultimate shear strength of plate elements with pit corrosion wastage", *Thin-Wall. Struct.*, **42**, 1161-76.
- Ok, D., Pu, Y. and Incecik, A. (2007), "Computation of ultimate strength of locally corroded unstiffened plates under uniaxial compression", *Mar. Struct.*, **20**, 100-114.
- Cyr, R.R.J. and Akhras, G. (2004), "Buckling of corroded stiffened steel plates", Proceedings of CSME, p.802-9.
- Akhras, G. and Cyr, R. (2004), "Testing corroded stiffened steel plates for ultimate strength", Proceedings of the fifth structural specialty conference CSCE, ST-188.
- Nakai, T., Matsushita, H. and Yamamoto, N. (2004), "Effect of pitting corrosion on local strength of hold frames of bulk carriers (2nd report). Lateral-distortional buckling and local face buckling", *Mar. Struct.*, **17**, 612-641.
- Dunbar, T.E., et al. (2004), "A computational investigation of the effects of localized corrosion on plates and stiffened panels", *Mar. Struct.*, **17**(5), 385-402.
- Amlashi, H.K.K. and Moan, T. (2005), "On the strength assessment of pitted stiffened plates under biaxial compression loading", 24th international conference on offshore mechanics and arctic engineering, Halkidiki, Greece.
- ANSYS Inc. (2008), "ANSYS 11.0 Reference Manual".
- Khedmati, M.R. (2000), "Ultimate strength of ship structural members and systems considering local pressure loads", Dr. Eng. Thesis, Graduate School of Engineering, Hiroshima University.
- Fujikubo, M., Yao, T., Khedmati, M.R., Harada, S. and Yanagihara, D. (2005), "Estimation of ultimate strength of continuous stiffened panel under combined transverse thrust and lateral pressure, Part 1: Continuous plate", *Marine Structures*, **18**, 383-410.
- Fujikubo, M., Harada, S., Yao, T., Khedmati, M.R. and Yanagihara, D. (2005), "Estimation of ultimate strength of continuous stiffened panel under combined transverse thrust and lateral pressure, Part 2: Continuous stiffened panel", *Marine Structures*, **18**, 411-417.
- Ueda, Y. and Yao, T. (1985), "The influence of complex initial deflection on the behaviour and ultimate strength of rectangular plates in compression", *J. of Const. Steel Research*, **5**, 265-302.
- Yao, T., Nikolov, P.I. and Miyagawa, Y. (1992), "Influence of welding imperfections on stiffness of rectangular plates under thrust", Proc. of IUTAM Sump. on Mechanical Effects of Welding, (Eds.: Karlsson, K., Lindgren, L.E. and Jonsson, M.), *Springer-Verlag*, 261-268.
- Ohyagi, M. (1987), "Statistical Survey on Wear of Ship's Structural Members", NK Technical Bulletin, Tokyo.
- Khedmati, M.R. and Karimi, A.R. (2006), "Ultimate compressive strength of plate elements with randomly distributed corrosion wastage", Proceeding of the Eight International Conference on Computational Structural Technology, (Eds.: Topping, B.H.V., Montero, G. and Montenegro R.), Civil-Comp Press.
- Ghavami, K. (1994), "Experimental study of stiffened plates in compression up to collapse", *J. of Const. Steel Research*, **28**(2), 197-222 [Special Brazilian Issue, Guest Editor Khosrow Ghavami].
- Ghavami, K. and Khedmati, M.R. (2006), "Numerical and experimental investigations on the compression behaviour of stiffened plates", *J. of Const. Steel Research*, **62**(11), 1087-1100.
- Fujikubo, M., Yao, T. and Khedmati, M.R. (1999), "Estimation of ultimate strength of ship bottom plating under combined longitudinal thrust and lateral pressure", *Trans. West Japan Soc. Nav. Architects*, 99.